ELSEVIER

Polymer 42 (2001) 2267–2273

polymer

www.elsevier.nl/locate/polymer

Polymer Communication

Stability of microdomain morphology in tethered block copolymer monolayers

I. Luzinov, D. Julthongpiput, V.V. Tsukruk*

Department of Materials Science and Engineering, Iowa State University, Ames, IA 50011, USA

Received 3 March 2000; received in revised form 5 June 2000; accepted 15 June 2000

Abstract

Robust and uniform ultrathin elastomeric films with complete surface coverage were fabricated from poly[styrene-*b*-(ethylene-*co*-butylene)-*b*-styrene] (SEBS) functionalized with 2% of maleic anhydride by grafting to a chemically modified silicon surface via epoxy-terminated self-assembling monolayers. We varied the thickness L of the SEBS film, from 1.4 to 8.5 nm, to test the limits of the stability of microphase-separated structures under confined conditions. We observed that the in-plane cylindrical/spherical microdomain morphology is similar to the bulk microstructure but it is compressed in vertical direction due to film–air and film–substrate interfacial constrains. Such a microstructure is formed at thicknesses in the range from 2.6 to 9 nm and is perfectly defined at $L/L_0 = 0.3$ (SEBS interdomain spacing, $L_0 = 28$ nm). Microphase separation is completely suppressed only for extremely thin films with $L/L_0 < 0.08$. Unlike physically adsorbed SEBS monolayers, which dewet the silicon surface, tethered block copolymer monolayers obtained under identical conditions are very stable even under high shear stresses and at elevated temperatures.

Keywords: Scanning probe microscopy; Polymer interface; Microdomain structure

1. Introduction

Thin films of block copolymers are currently under intensive study [1–10]. Their ability to form coatings with exceptional characteristics due to their unique microdomain morphology is of great interest [1,4,7,11,12]. These films undergo a series of structural reorganizations of the surface microdomain morphology depending upon the L/L_0 ratio, where L is the film thickness and L_0 the equilibrium spacing of the microdomain structure [1–3,9,10]. A great deal of work in this area is devoted to the ABA block copolymers where A constitutes thermoplastic materials (e.g. polystyrene) and B is an elastomer (e.g. polybutadiene or ethylene/butylenes copolymer). These triblock copolymers are capable of forming thermoplastic elastomer (TPE) coatings [5–8].

Van Dijk and van den Berg [5] studied thin films of poly[styrene-*b*-butadiene-*b*-styrene] (SBS) block copolymer with thickness ranging from 30 to 150 nm. It was found that the films possess a cylindrical microstructure close to the one observed for the bulk materials with different PS cylinder orientation that depends upon the average film thickness. Motomatsu et al. [8] studied the poly[styrene-*b*-(ethylene-*co*-butylene)-*b*-styrene] (SEBS) triblock copolymer film with $L = 170$ nm. The surface of the film exhibited characteristic cylindrical morphology similar to the bulk microstructure.

In general, researchers limit their studies to relatively "thick" films from block copolymers with $L > 30$–100 nm that corresponds to the regime $L/L_0 > 1$ or film thicknesses higher than the equilibrium interdomain spacing. Scaling down the thickness to the limit $L/L_0 < 1$ is a challenging task. When the film thickness is bellow L_0, the morphology of the film is disturbed by the competition of several forces, including strong surface interaction, slow kinetics, and the "bulk" driving force towards a morphology with natural period L [13]. As a result, several morphologies were observed for block copolymer ultrathin films. Russel et al. [14] reported the formation of micron size islands with a step height L_0. Harrison et al. [15] observed that the SBS film, with a thickness of 20 nm, deposited on polystyrene brush-coated wafers produced a "zeroth" layer, which does not demonstrate the microdomain morphology. The formation of a random array of uniformly sized circular domains was observed for the poly(styrene-*b*-butyl methacrylate) diblock copolymer film (thickness ~30 nm) [13]. The general conclusion is that when the thickness of the

* Corresponding author. Tel.: +1-515-294-6904; fax: +1-515-294-5444.
E-mail address: vladimir@iastate.edu (V.V. Tsukruk).

0032-3861/01/$ - see front matter
PII: S0032-3861(00)00461-4

deposited film approaches equilibrium interdomain spacing, the microphase separation is disturbed and further reduction of film thickness results in inhomogeneous surface coverage. To the best of our knowledge, *stable and uniform* ultrathin films from thermoplastic elastomer copolymers with complete surface coverage and developed microdomain structure at thickness well below the interdomain spacing has not yet been demonstrated.

To test this conclusion for the SEBS block copolymer studied in this work, we fabricated very thin polymer films (overall thickness measured by ellipsometry is less than 3 nm) on a bare silicon surface under identical experimental conditions described below. As we observed, indeed, these films are incomplete or possess island morphology (Fig. 1) that confirms the paradigm known for block copolymer films. Therefore, a different approach should be thought to prevent this natural tendency. Very minor variation of deposition conditions leads to dramatic reconstruction of film morphology due to the inherit instability of film at $L \ll L_0$.

In this communication, we focus on the fabrication of uniform and robust ultrathin block copolymer layers with $L/L_0 \ll 1$ (the thickness below 10 nm) via chemical grafting of the polymer to the reactive interface. This regime is very interesting from the point of view of prospective nanotechnology applications of block copolymers for submicrometer photolithography and molecular lubrication for microelectromechanical systems where space constrains require robust coatings with thickness less than 5–10 nm [1,4,16–19]. We tested the limits of the stability of the microdomain morphology under these very space-restrictive conditions. In this work, we demonstrated that uniform and robust nanometer thick films from block copolymers, indeed, can be fabricated if an appropriate anchoring strategy is used. We observed that these films show very uniform surface composition, are very smooth, demonstrate no sign of island microstructure even under severe thermal treatment, and are extremely stable and robust under shear stresses.

To avoid the dewetting and stabilize of ultrathin films with nanometer scale thickness or $L/L_0 \ll 1$, we grafted functionalized ABA triblock copolymer on a specially prepared chemically reactive silicon surface. The triblock copolymer was poly[styrene-*b*-(ethylene-*co*-butylene)-*b*-styrene] (SEBS) functionalized with 2% of maleic anhydride (MA) randomly imbedded into the hydrocarbon chains. The epoxy-terminated self-assembled monolayer (SAM) deposited on a silicon wafer prior block copolymer layer fabrication was used as a reactive anchoring surface. We showed previously that for these homogeneous and robust SAMs, terminal epoxy groups were mainly located at the surface [20,21].

2. Experimental

The procedure of epoxy-terminated SAM fabrication on silicon wafers is described in detail elsewhere [20,21]. The SEBS studied here is Kraton 1901 (Shell) with styrene and maleic anhydride contents of 29 and 2 wt%, respectively. The molecular weight measurements were carried out for the SEBS solution in THF using a Waters-GPC equipped with Mini Dawn (Wyatt Technology) light scattering detector. GPC data showed $M_n = 41,000$ g/mol, $M_w/M_n = 1.16$, and $R_g = 6.3$ nm, where R_g is the radius of gyration of SEBS macromolecules. The SEBS copolymer layer was deposited on the epoxy-terminated SAM from toluene solution and melt. The MA groups of the elastic block (PEB) react with the epoxy groups of the monolayer [22], thus enabling anchoring of the elastic block to the surface.

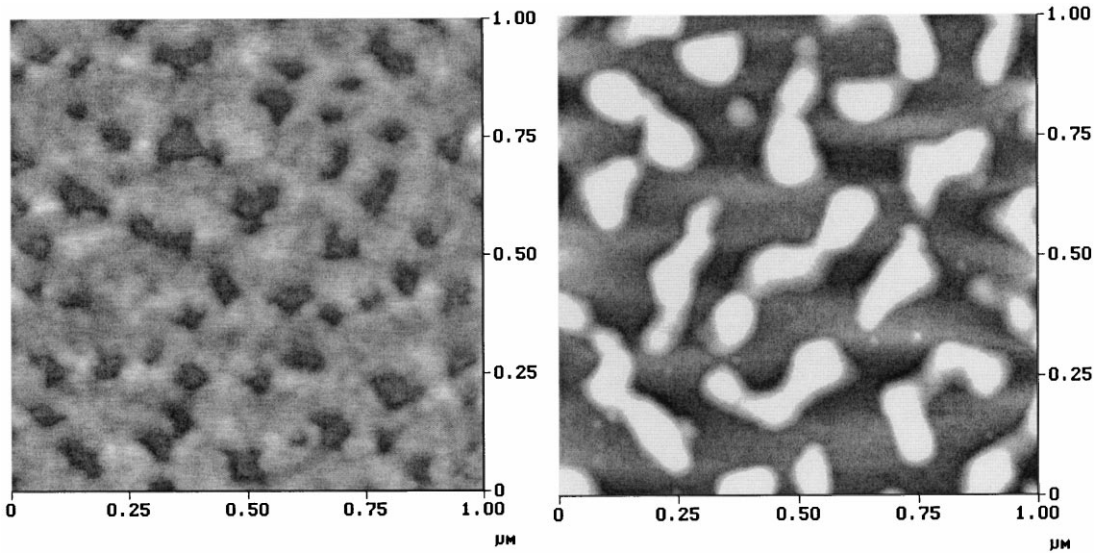

Fig. 1. Different morphologies observed for SEBS film with thickness of about 3 nm obtained by adsorption from solution on a bare silicon wafer under variable conditions similar to the grafting procedure. Vertical scale is 20 nm. Bright parts correspond to higher features.

For grafting from the solution, the SAM modified silicon wafer was immersed in the polymer solutions of different concentrations (from 0.25 to 8 wt%) for 24 h. For grafting from the melt, the initial polymer film was spin-coated from the 1.5 wt.% toluene solution. The initial thickness of the spin-coated film measured by ellipsometry was 60 ± 6 nm. The specimens were placed in a vacuum oven at 150°C for 45 min to enable the MA groups to react with the epoxy-terminated SAM. The unbounded polymer was removed by multiple washing with toluene, including the washing in an ultrasonic bath. The film surfaces were examined by a static contact angle (sessile droplet) using a custom-designed optical microscopic system. Ellipsometry was performed with a COMPEL automatic ellipsometer (InOmTech, Inc.). Scanning probe microscopy (SPM) was done on a Dimension 3000 (Digital Instruments, Inc.) microscope according to the experimental procedure described in detail earlier [23].

To characterize the grafted film, several parameters have been evaluated [24]. The surface coverage, Γ (mg/m^2), was calculated from the ellipsometry and SPM thickness of the layer h (nm) by the following equation:

$$\Gamma = h\rho \tag{1}$$

where $\rho = 0.905$ g/cm^3 is density of SEBS. The density of SEBS was estimated from the density of polyethylene in rubbery form and polystyrene in glassy form by additive approximation [25]. The grafting density, Σ (chain/nm^2), i.e. the inverse of the average area per adsorbed chain was determined by:

$$\Sigma = \Gamma N_A \times 10^{-21}/M_n = (6.023\Gamma \times 100)/M_n \tag{2}$$

where N_A is Avogadro's number and M_n (g/mol) is the number average molecular weight of the grafted polymer.

3. Results and discussion

Fig. 2a demonstrates the thickness of SEBS film grafted from solution versus its concentration. The layer height gradually increases to 2.7 nm for 8% concentration. Grafting from the melt results in much thicker film ($L = 8.5$ nm). For the grafting conditions used, the surface coverage (Γ) and grafting density (Σ) vary from 1.2 to 7.6 mg/m^2 and from 0.019 to 0.12 chain/nm^2, respectively (Fig. 2b). These values are very close to the grafting parameters obtained for PS of comparable molecular mass grafted to epoxy-terminated SAMs [26].

Fig. 2a shows the thickness of the films scaled with the interdomain spacing, L_0. In our estimations, we use $L_0 =$ 28 nm, since this value is reported for similar SBS block copolymer with very close composition [27,28]. The combination of the grafting from the melt and solution allows us to vary the film thickness in a wide range of L/L_0 from 0.05 to 0.3, thus, keeping the target condition for ultrathin film, $L/L_0 \ll 1$.

Fig. 2c presents the contact angle for SEBS films. The contact angle varies from 93° for the thinnest film to 100 ± 2 for $L > 1.7$ nm. These values are within the range reported for PS surface (90°) [29] and polyethylene surface (99 ± 3°) [30]. Since the chemical composition and surface energies of polyethylene and polybutylene are very close [25], for their copolymer, PEB, we can expect the contact angle to be close to 99°. Therefore, contact angle measurements show that PEB chains completely cover the film surface at thickness $t > 1.7$ nm. This observation is consistent with other investigations, which demonstrated that the surface of a monolayer thick block copolymer film is covered with a component with lower surface energy [15,31].

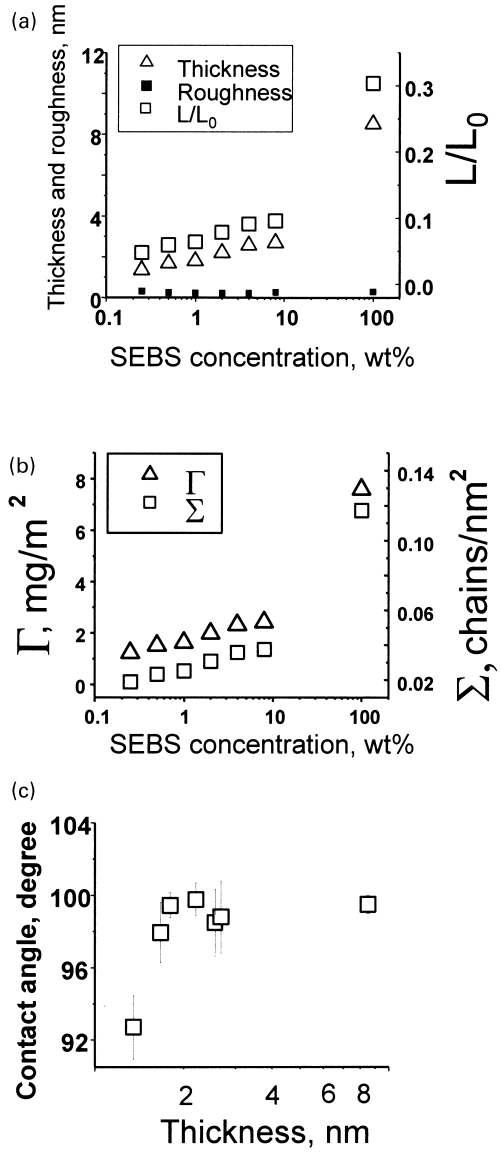

Fig. 2. (a) SEBS film thickness as measured by ellipsometry, SPM microroughness and the film thickness reduced to L_0 (interdomain spacing) versus concentration of SEBS in solution and melt. (b) Surface coverage, Γ (mg/m^2) and grafting density, Σ (chain/nm^2) versus concentration of SEBS in solution and melt. (c) Water contact angle for the SEBS film versus the thickness of the film.

SPM imaging provides further insight into the film microstructure (Figs. 3 and 4). First of all, it shows that all films are uniform without islands, holes, and dewetting areas, unlike physically adsorbed SEBS films of comparable thickness (Fig. 1). The film surface is very smooth as indicated by the microroughness within the 1 μm × 1 μm area in the range of 0.2–0.3 nm (Fig. 2a).

The free amplitude for scanning probe, A_0, was chosen to be about 40 nm. For "light" and "hard" tapping modes, the set-point amplitude ratio, $r_{sp} = A_{sp}/A_0$ (A_{sp} is the set-point amplitude used for the feedback control), was selected to be 0.9 ± 0.05 (amplitude damping of 4 nm) and 0.45 ± 0.05 (amplitude damping 22 nm), respectively. The amplitude and phase variation show that, at $r_{sp} > 0.85$, we scanned at an attractive interaction regime. The repulsive mode was in place at $r_{sp} = 0.45$.

Fig. 3 presents topographical and phase images of the SEBS films recorded at the highest set point ($r_{sp} = 0.9 \pm 0.05$) or the lowest forces applied. Fig. 4 shows SPM images from the same films recorded with the low set point ($r_{sp} = 0.45 \pm 0.05$) or high forces applied. According to SPM studies on similar block copolymers [6], under these conditions, the topographical images in Fig. 3 reflect the morphology of the topmost layer and phase imaging is controlled by surface adhesion. In contrast, the SPM images in Fig. 4 are recorded in the repulsive mode and a major contribution comes from the elastic response of the film. Under these scanning conditions, the SPM tip squeezes the topmost rubbery layer and interacts with hard domains.

For the SEBS layers with thickness $L < 2.2$ nm ($L/L_0 < 0.08$), the SPM images show very fine, random nanoscale texture (Fig. 3a and b). When the SEBS film reaches 2.6 nm ($L/L_0 = 0.1$), the first evidence for the microphase separation of PS within the film was detected (image not shown). We observed tiny circular domains of PS randomly distributed on the surface. For the film with 8.5 nm thickness ($L/L_0 = 0.3$), the SPM images show the microdomain structure typical for the analogous block copolymer films [5–8]

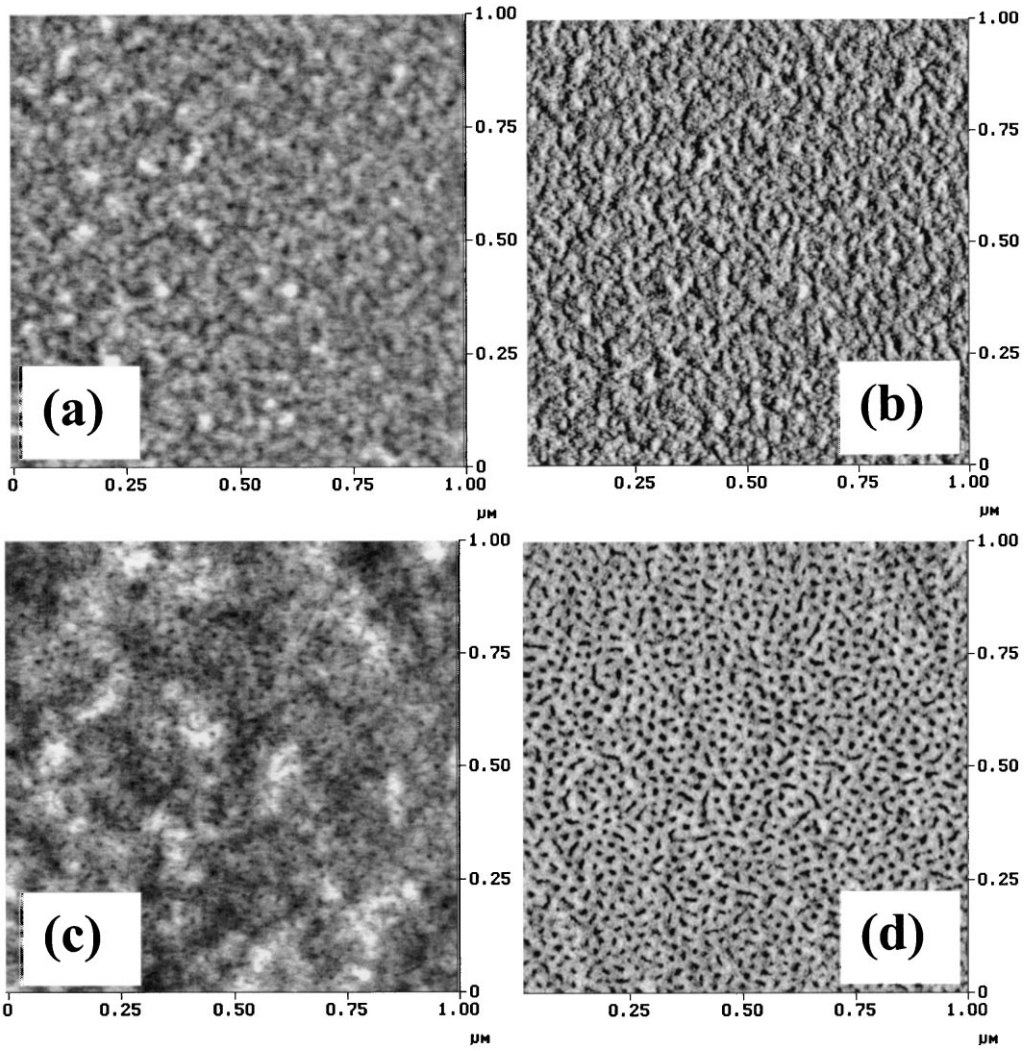

Fig. 3. SPM topographical (a and c) and phase (b and d) images of SEBS films with thickness 1.8 (a, b) and 8.5 nm (c, d). Vertical scale is 7.0 nm and 20° for topography and phase modes, respectively. Bright parts correspond to higher features and phase shifts. "Light" tapping.

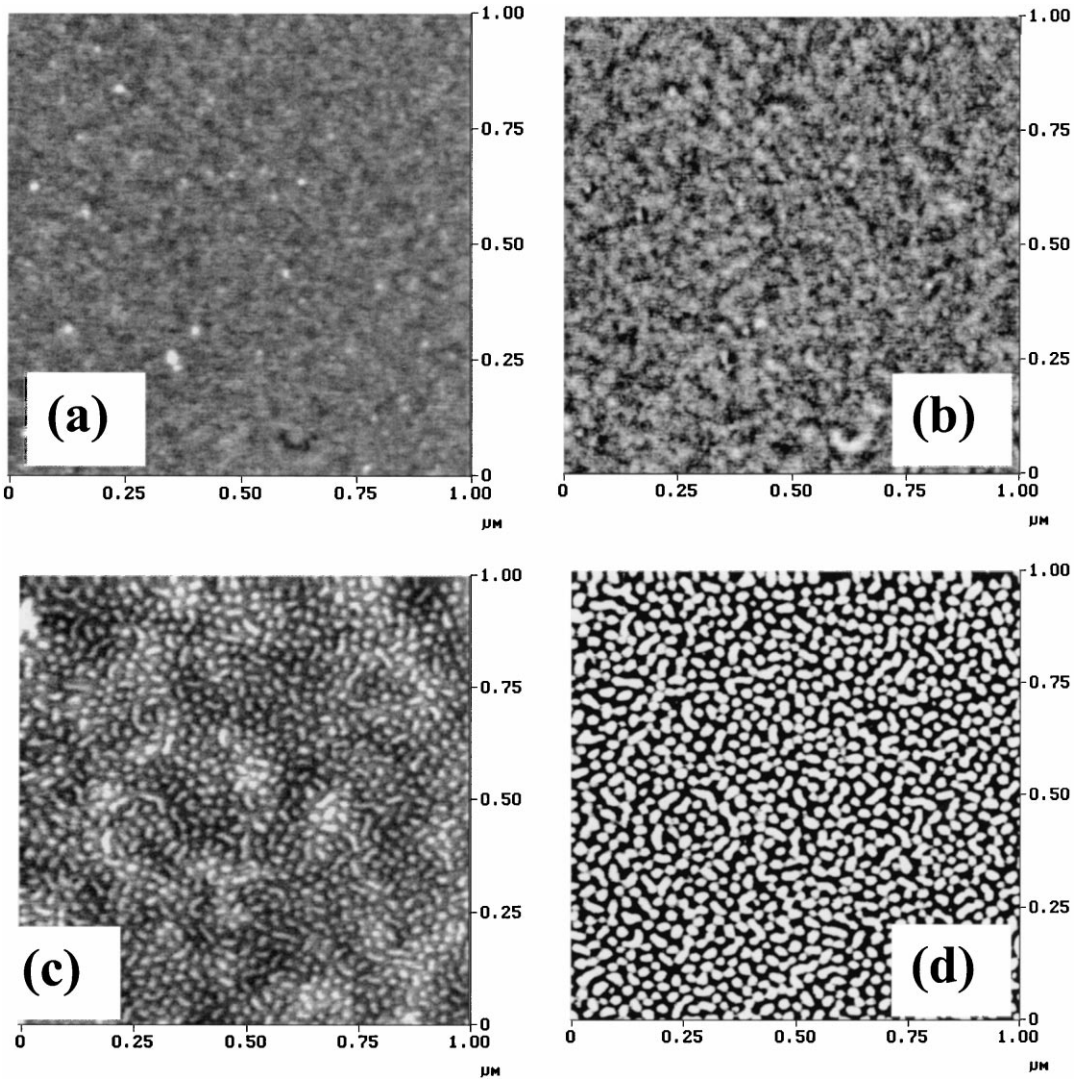

Fig. 4. SPM topographical (a and c) and phase (b and d) images of SEBS films with thickness 1.8 (a and b) and 8.5 nm (c and d). Vertical scale is 7.0 nm and 100° for topography and phase modes, respectively. Bright parts correspond to higher features and phase shifts. "Hard" tapping.

(Fig. 3c and d). We observe a mixture of spherical and cylindrical PS domains with an apparent diameter less than 12 nm. Modest widening is present due to the SPM tip dilation and can be estimated as contributing 20–30%, thus leading to better estimation of the actual diameter as less than 10 nm. The average spacing in short-range ordered microdomains is 28 ± 2 nm as determined from the 2D Fourier-transformation. Close parameters of the microdomain structure are deducted from SPM data recorded in repulsive mode. The pronounced difference is reverse contrast on the phase images of microdomain structures (compare Figs. 3d and 4d). This change is purely instrumentation appearance related to the change of a phase shift at the transition from attractive to repulsive mode as discussed in detail in Ref. [6].

The in-plane SEBS microdomain structure within ultrathin layers (30% of equilibrium spacing and 70% of unperturbed macromolecular diameter) is *very similar* to the one observed in thick films and bulk [7,8]. The interdomain distances, L_0, and domain diameter, r, are virtually non-distinguishable in the molecular film and in the bulk: $L_0 = 28 \pm 2$ nm in comparison to 27–30 nm and $r <$ 10 nm in comparison to 9–10 nm, respectively. However, we should assume that at least 1–2 nm below and 1–2 nm above the PS microphase is occupied by the PEB block to provide tethering to SAMs and cover the film surface (in accordance with our observations). Thus, only a 5–6 nm thick layer is left for the PS phase itself, which immediately concludes the *compressed shape* of the PS domains within this film along the surface normal.

This leads us to the model with compressed spherical and cylindrical PS microdomains (Fig. 5). The MA units of the grafted SEBS, which are not attached to the epoxy-terminated SAM, should be randomly distributed within the grafted film. Apparently in thin films, the chemical grafting of the rubber block to the surface prevents the formation of

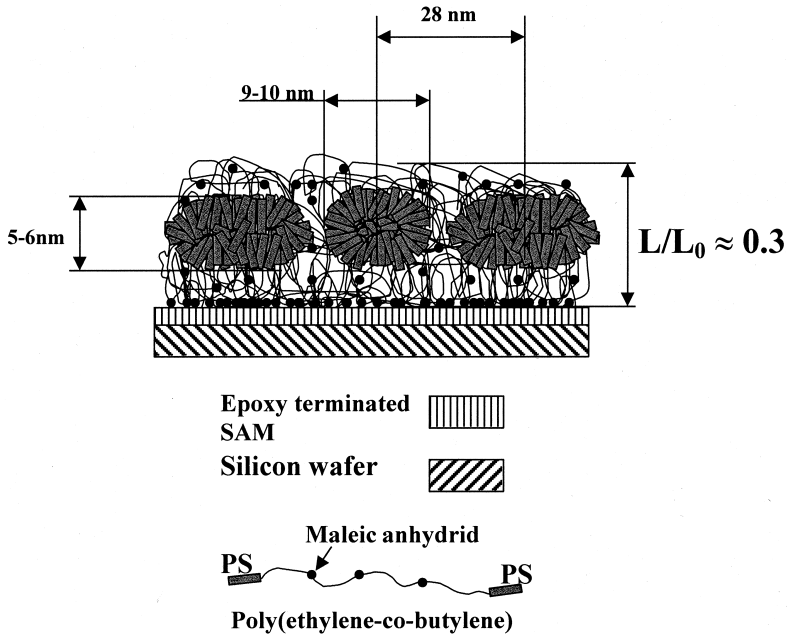

Fig. 5. Schematic representation of the SEBS monolayer microstructure.

well-developed in-plane cylindrical microstructure with compressed domains due to space constrains imposed by air–film and film–substrate interfaces.

Finally, we tested the thermal and mechanical stabilities of the grafted films (detailed results will be published elsewhere [32,33]). The grafted and spin-coated films with close thicknesses (8.5 and 10 nm) were annealed for 7 h in a vacuum oven at 150°C and compared. As we observed, the microdomain microstructure in the grafted film remains unchanged after the thermal treatment. On the other hand, the spin-coated film showed significant surface corrugation (image not shown) [33]. Highly heterogeneous surface morphology was developed with microroughness increasing to 1 nm. Finally, by using the wearing SPM test [21], we observed that the grafted SEBS film was extremely robust and sustained shear stresses many times higher than for similar SEBS films deposited on bare silicon (for details see Ref. [32].

Acknowledgements

This work is supported by The National Science Foundation, CMS-9996445 Grant. The authors thank P.D. Bloom and E.C. Hagberg for GPC measurements and Shell Co. for donating the SEBS sample.

References

[1] Huang E, Russell TP, Harrison C, Chaikin PM, Register RA, Hawker CJ, Mays J. Macromolecules 1998;31:7641.
[2] Mansky P, Russell TP, Hawker CJ, Pitsikalis M, Mays J. Macromolecules 1997;30:6810.
[3] Liu Y, Rafailovich MH, Sokolov J, Schwarz SA, Bahal S. Macromolecules 1996;29:899.
[4] Meiners JC, Quintel-Ritzi A, Mlynek J, Elbs H, Krausch G. Macromolecules 1997;30:4945.
[5] Van Dijk MA, van den Berg R. Macromolecules 1995;28:6773.
[6] Magonov SN, Cleveland J, Elings V, Denley D, Whangbo M-H. Surf Sci 1997;389:201.
[7] Kim G, Libera M. Macromolecules 1998;31:2569.
[8] Motomatsu M, Mizutani W, Tokumoto H. Polymer 1997;38:1779.
[9] Foster MD, Sikka M, Singh N, Bates FC, Satija SK, Majkrzak CF. J Chem Phys 1992;96(11):8605.
[10] Koneripalli N, Singh N, Levicky R, Bates FC, Gallagher PD, Satija SK. Macromolecules 1995;28:2897.
[11] Xie R, Karim A, Douglas JF, Han CC, Weiss RA. Phys Rev Lett 1998;81:1251.
[12] Liu Y, Rafailovich MH, Sokolov J, Schwarz SA, Zhong X, Eisenberg A, Kramer EJ, Sauer BB, Satija S. Phys Rev Lett 1994;73:440.
[13] Fasolka MJ, Harris DJ, Mayes AM, Yoon M, Mochrie SGJ. Phys Rev Lett 1997;79:3018.
[14] Russell TP, Mayes AM, Bassereau P. Physica A 1993;200:713.
[15] Harrison C, Chaikin PM, Huse DA, Register RA, Adamson DH, Daniel A, Huang E, Mansky P, Russel TP, Hawker CJ, Egolf DA, Melnikov IV, Bodenschatz E. Macromolecules 2000;33:857.
[16] Ndoni S, Jannasch P, Larsen NB, Almdal K. Langmuir 1999;15:3859.
[17] Mansky P, Harrison CK, Chaikin PM, Register RA, Yao N. Appl Phys Lett 1996;68:2586.
[18] Bliznyuk VN, Everson MP, Tsukruk VV. J Tribology 1998;120:489.
[19] Tsukruk VV, Nguyen T, Lemieux M, Hazel J, Weber WH, Shevchenko VV, Klimenko N, Sheludko E. In: Bhushan B, editor. Tribology issues and opportunities in MEMS. Dordrecht: Kluwer Academic, 1998. p. 608.
[20] Tsukruk VV, Luzinov I, Julthongpiput D. Langmuir 1999;15:3029.
[21] Luzinov I, Julthongpiput D, Liebmann-Vinson A, Cregger T, Foster MD, Tsukruk VV. Langmuir 2000;16:504.
[22] May CA, editor. Epoxy resins: chemistry and technology. New York: Marcel Dekker, 1988.

[23] Tsukruk VV. Rubber Chem Tech 1997;70(3):430.
[24] Henn G, Bucknall DG, Stamm M, Vanhoorne P, Jerome R. Macromolecules 1996;29:4305.
[25] Van Krevelen DW. Properties of polymers. 3rd ed. Amsterdam: Elsevier, 1997 (chap. 8).
[26] Luzinov I, Julthongpiput D, Malz H, Pionteck J, Tsukruk VV. Macromolecules 2000;33:1043.
[27] Helfand E, Wasserman ZR. Macromolecules 1976;9:879.
[28] Helfand E, Wasserman ZR. Macromolecules 1978;11:960.
[29] Luzinov I, Minko S, Senkovsky V, Voronov A, Hild S, Marti O, Wilke W. Macromolecules 1998;31:3945.
[30] Price GJ, Clifton AA, Keen F. Polymer 1996;37:5825.
[31] Mansky P, Chaikin P, Thomas EL. J Mater Sci 1995;30:1987.
[32] Luzinov I, Julthongpiput D, Gorbunov V, Tsukruk VV. Trib Int 2000 (submitted).
[33] Luzinov I, Julthongpiput D, Tsukruk VV. Macromolecules 2000 (accepted).